Journal of Sound and Vibration 365 (2016) 89–101

Contents lists available at ScienceDirect

Journal of Sound and Vibration

journal homepage: www.elsevier.com/locate/jsvi

A precise non-destructive damage identification technique of long and slender structures based on modal data

Martin Stache*, Marcus Guettler, Steffen Marburg

Technische Universität München, Department of Mechanical Engineering, Vibroacoustics of Vehicles and Machines, Boltzmannstrasse 15, 85748, Garching bei München

ARTICLE INFO

Article history:
Received 1 March 2015
Received in revised form
2 December 2015
Accepted 4 December 2015
Handling Editor: I. Trendafilova
Available online 21 December 2015

Keywords:
Modal Analysis
Finite-Element-Method
Eigenfrequency
Non-Destructive-Testing
Damage Identification

ABSTRACT

This paper presents numerical and experimental studies on modal behavior of cylindrical, lightly damped beam structures containing a notch-like crack with variable position and geometry. The numerical investigation utilizes the Finite-Element-Method (FEM) and a discretization strategy is developed that enables a crack to be represented in three dimensions. A test procedure capable of delivering a broadband impulse excitation to a flexible supported test specimen was developed. The customized excitation unit was used in conjunction with a Laser-Scanning-Vibrometer (LDV) to analyze a frequency range up to 40 kHz. The first 15 bending mode shape pairs with their corresponding eigenfrequencies are numerically and experimentally identified. The model updating is performed for the elastic parameters and the boundary conditions to minimize the deviation between experimentally determined and numerically calculated results in terms of eigenfrequencies. The acquired data are used in a two-stage damage identification procedure, in which suitable start vectors are found by the evaluation of objective function plots. Subsequently, geometrical crack parameters are identified. The deviations between real and determined crack positions range between 0.05 and 0.28 percent for crack depth/diameter ratios of less than 7 percent.

1. Introduction

The engineering field of damage identification based on modal data is well represented in the literature [5–8,20]. Defects change the geometry and the mechanical properties of structures and cause a measurable modification of their dynamic behavior in relation to an undamaged system. Damage identification based on modal data has diverse applications in structural health monitoring (SHM), condition monitoring (CM) and non-destructive testing (NDT).

Focusing on non-destructive testing, classical inspection techniques require the section of interest to be accessible. Due to their local character, the data extraction is slow in comparison to global techniques. By definition, using non-destructive methods one is capable of evaluating structural integrity without disturbing the structure's future performance. Common methods are based on visual observations or the analysis of changes in material properties. The method presented in this paper uses changes in the global behavior of the observed structure to interpret the structural condition. The modal parameters of a structure, such as the eigenfrequencies, mode shapes and modal damping, are functions of the structure's

* Corresponding author.
E-mail address: martinstache@gmx.de (M. Stache).

http://dx.doi.org/10.1016/j.jsv.2015.12.013

physical properties and type of support. Hence, changes in physical properties such as mass, stiffness and damping will result in a change in modal properties. For the case of a crack, local lowering of stiffness occurs which causes a change in modal properties that can be determined experimentally.

In general, vibration based techniques involve the application of an excitation to the observed structure as well as the interpretation of the structural response at various locations. The process of modal identification can be discussed in terms of observability and identifiability [22–24].

Inherent features of structures often exhibit unknown parameters. One possibility to estimate these parameters is to observe the structures' input–output behavior. A given structure possesses an unknown system state with the controllable input and the observable output. The physics of the structure are characterized by the system properties. For observability, the aim is to determine whether mathematical relations exist between the unknown system state and the input/output quantities [25–27]. Therefore, the information content of the measurement data must be sufficient to conclude the state of the observed structure. In this context, appropriate test parameters play a central role, such as the frequency range of interest, sensor positions as well as the number of measurement points. Identifiability represents a special case of the observability problem, in which system properties can be uniquely described by the input and the output [28,29].

Regarding the numerical analysis, requirements on the structure model like type of elements and mesh refinement have to be determined, which mainly influence the precision of the computed data.

Testing methods based on the alteration of eigenfrequencies are concerned with global structure behavior and therefore enjoy faster data extraction than classical local methods such as ultrasonic testing. Disadvantages of these global methods are often mentioned in terms of the non-uniqueness of the results [1,2]. It is commonly known that especially in axi-symmetric parts, the results of damage position are generally ambiguous. Thereby, the crack possesses at the minimum two potential positions, when only eigenfrequency information is used. One approach to overcome this drawback is to connect global methods with local methods, such as in multi-criterion optimization. Herein, eigenfrequency-based data is combined with highly resolved local information in the form of eigenvectors.

Despite the well-founded scientific knowledge of vibration based damage identification, concrete information regarding the results' precision is sparsely published. Neither investigations have been realized that describe the successful identification of damage scenarios smaller than 10 percent with respect to the cross-sectional area. The following reasons present possible explanations:

- eigenfrequencies possess high dependency on geometric part tolerances. It is difficult to differentiate between damage-induced and tolerance-induced alterations (e.g. changes in diameter, length and circularity),
- small damage levels have less effect on the eigenfrequencies of lower rank,
- due to the high modal density and the resonance overlapping of highly damped materials, it is difficult to perform measurements at high frequencies,
- nonlinear dynamic behavior must be linearized and
- test conditions such as support, excitation and equipment settings are difficult to reproduce.

In this paper a damage identification technique is presented using numerically calculated and experimentally determined eigenfrequencies of nine test objects with different crack positions and depths. The first 15 mode shape pairs are identified in a frequency range up to 40 kHz. First, the Finite-Element (FE) models of cylindrical structures, containing a crack at different positions and with different depths, are investigated. In a second step, the test objects' specimens with analogous geometry to the numeric models are analyzed by the use of a Laser-Doppler-Vibrometer (LDV). Wire erosion is utilized to ensure precise crack geometry. In the last step, the numerical and experimental data is applied to a damage identification procedure in which crack position and size are determined.

The damage identification procedure developed in this work relies on the minimization of an eigenfrequency-based objective function. This objective function compares the numerical modal data of a parametric model with corresponding data from an experimental modal analysis. Geometric crack parameters of the numerical model are modified until the eigenfrequency-based objective function is converged. Only bending mode shapes are considered. This limitation is made for reasons of convenient support and excitation conditions. The crack is assumed to be open and therefore the width is set to a reasonable extent. Bi-linear effects [21] due to closing crack sites are neglected. Moreover the crack width is defined as constant to avoid mass-induced changes of eigenfrequencies over the identification process. For the experimental investigation a shaker with a high dynamic range is used to excite the system. The test specimens are elastically supported at both ends. Numerically an elastic foundation is modeled to consider realistic boundary conditions.

The focus of this paper is on the development of converged numerical models using a mixed element mesh in combination with highly accurate experimental data, which both directly influence the predictive accuracy of the implemented damage identification procedure. The achieved precision provides the ability of identifying crack depth/diameter ratios of less than 7 percent, which is novel among the available literature. For a fast and stable optimization procedure an innovative precondition routine is introduced, in which suitable start parameters are compiled by using one-time generated objective function plots.

2. The physical problem

A crack in a beam causes a local reduction of area moment of inertia. This reduction is equivalent to a decrease in local stiffness and results in a change of eigenfrequency values. This change in eigenfrequency-values increases, if the damage is positioned in cross-sections of high bending moments where mode shape curvature raises or if the damage size increases. For this reason, a large crack near a vibrational node can influence a single eigenfrequency of the observed mode to the same extent as a small crack positioned at an antinode [3,4]. To overcome this fact, it is suggested to observe at least two consecutive eigenfrequencies in the intended identification procedure. Further, for bending modes of rotationally symmetric structures, one eigenfrequency of a mode shape pair is less affected by the introduced asymmetric crack than the other. Consequently one eigenfrequency of the mode shape pair changes less and a splitting of eigenfrequency pairs can be observed.

3. Damage identification

In a damage identification numerically calculated and experimentally determined modal data are compared to compute geometrical defect parameters such as position and/or severity. Thereby, the outcome of the damage identification can only be as precise as the underlying data.

Based on the complexity of the optimization in this study, a numerical consideration is inevitable. The optimizer searches for the minimum of the objective function in a limited search space. In many applications of damage identification, the presence of several local minima complicates the identification of the global minimum [19]. Furthermore, modal features have to be selected carefully. Only modal data that are sensitive to the particular damage pattern can be used to accurately determine the crack parameters. The success of the damage identification procedure strongly depends on the choice of appropriate initial values for the searched defect parameters in the optimization process. Trial and error often results in convergence against the bounds of the search space which is not a useful output or in a high quantity of iterations.

The formulated numerical optimization problem in the present work is nonlinear. An optimization is mathematically defined as the minimization of an objective function. Mathematically this can be expressed by

$$\min\left\{f(\vec{\vartheta})\right\}, \quad \vartheta \in \mathbb{R}^n, \tag{1}$$

in which $\vec{\vartheta}$ describes the vector of the design or search parameters. Explicit restrictions [15] are placed on the design variables ϑ_i to bound them between lower ϑ_i^L and upper ϑ_i^U limits, defined as

$$\vartheta_i^L \le \vartheta_i \le \vartheta_i^U; \quad i = 1, n. \tag{2}$$

3.1. Approximation

In this study, a local approximation method is used to calculate new values for the crack parameters. The results of local methods are only valid in the vicinity of the actual design point [15]. However, these methods are able to reduce the total number of FE analyses required during the optimization. A local approximation method reformulates the optimization into the solution of a sequence of subproblems. The local approximation is achieved using the Method of Moving Asymptotes (MMA) [16], which has been successfully applied to other structural dynamic problems [17,18,30]. The objective function to be minimized consists of a quadratic error sum, built between the experimentally determined and numerically calculated eigenfrequencies, as follows:

$$f(\vartheta) = \sum \frac{(f_{\exp_i} - f_{\mathrm{num}_i})^2}{f_{\exp_i}^{\ 2}}. \tag{3}$$

To avoid adverse value ranges, both the objective function and the design parameters are scaled.

3.2. Identification routine

The suggested identification routine uses a two-stage optimization strategy. This serves for the identification of proper initial values, introducing the following two consecutive steps:

1. exhaustive search for suitable initial parameters on a course gridded objective function plot and
2. optimization by using the MMA.

A parametric model of the structure was generated that would automatically create the geometry and FE mesh for a given set of parameters, i.e. crack depth t and crack position y_0. Maintaining the physical consistency and avoiding mesh distortion, the model parameters change within an adequate interval. Crack depth t ranges between 0.2 and 1.75 mm, and

crack position y_0 between 15 and 285 mm. Element specification for the numerical models used in the damage identification are presented in Table 3.

In the process of damage identification a two-step procedure similar to the one suggested in [32] is developed. The first step aims to identify suitable initial values for the crack depth and position parameters by compiling coarse objective function plots. In the second step, these initial values are used to precondition the identification routine, which results in a fast and stable convergence.

For the objective function plots the calculation of eigenfrequencies in Abaqus is performed only once for all possible combinations of parameters (y_0 and t). The step size for the crack position and depth are 5 mm and 0.1 mm, respectively. Subsequently, the user is able to visualize the plots for all feasible eigenfrequency combinations involving the one-time experimentally determined eigenfrequencies of the real test specimens. In the light of the intended application of non-destructive testing, the suitability of all potential eigenfrequency combinations can be evaluated in a fast and efficient manner. Further, the parameter vector with the smallest deviation of objective function is used as the initial parameter vector for the optimization.

In the optimization process Python™ is used as the coding language to connect Abaqus with the external MATLAB-based optimizer. The first step consists in defining the initial values for crack position y_0 and depth t as well as the increment size for these crack parameters. Also the eigenfrequencies to be included in the objective function are selected. In the second step, Abaqus starts successively one objective function and two gradient analyses. The resulting eigenvectors and eigenfrequencies are saved to an output file. The third step contains the modal reduction and tracking and aims to compare the experimentally determined and numerically calculated eigenfrequencies of the same mode shapes. From these eigenfrequency values, the objective function and its gradients are calculated and provided to the external optimizer. In the fourth step, the optimization algorithm starts, which results in a new vector of parameters that is used for the next iteration. The optimization stops once the objective function drops below a predefined convergence criterion, or when a maximum number of iterations are reached.

4. Numerical investigations

The structures studied in this work are circular cylinders with a length $l=300$ mm and a diameter $d=6$ mm, as shown in Fig. 1. y_0 represents the position of the crack and t its depth. The crack width w is 0.5 mm and constant over the nine models. The material is modeled using HOOKE's isotropic elastic material model. Table 1 presents the parameters of HOOKE's material model.

The numerical analyses are conducted using the commercial software Abaqus. On the one hand the presented discretization strategy considers that large stress gradients due to the crack geometry must be dissolved. On the other hand the ability to parameterize the structural model enables an automated optimization procedure, which will be discussed later.

Table 2 presents the geometrical crack parameters of the crack models analyzed. Crack depth/diameter ratios of 25.00 percent, 12.50 percent and 6.25 percent which correspond to cross section ratios (damaged/undamaged) of 19.55 percent, 7.22 percent and 2.60 percent are investigated.

Fig. 2 shows the numerical model used for the cylinders. The model is divided into three partitions: two 'crack-free' partitions at either end of the cylinder and a 'crack' partition which includes the region around the crack.

The crack-free partitions are discretized with second-order 20-node brick elements with reduced integration [9]. To avoid mesh distortion, the crack partition is additionally modeled with second-order 15-node wedge elements. In comparison to the undamaged partitions, the cracked partition is meshed with a mesh density twice as large as in the undamaged region, in order to resolve the stress gradients caused by the crack geometry. The connections between the partitions of different mesh densities and different element types are realized using tie-constraints, which couple the nodal degrees of freedom of adjacent nodes in the interface area [9,14].

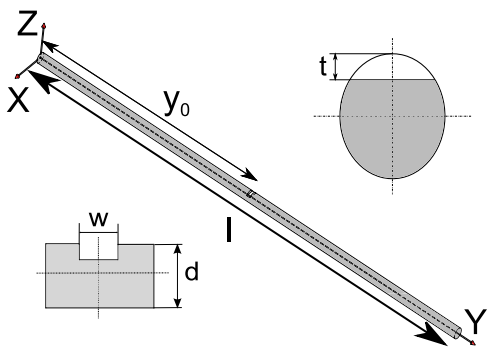

Fig. 1. Parametric model for damage identification.

Table 1
Parameters of Hooke's material model.

Density	Young's modulus	Poisson ratio
14,450 kg/m^2	566.5 GPa	0.19

Table 2
Geometrical parameters of the crack models.

Model	1	2	3	4	5	6	7	8	9
w (mm)	0.5	0.5	0.5	0.5	0.5	0.5	0.5	0.5	0.5
y_0 (mm)	150.0	150.0	150.0	75.0	75.0	75.0	37.5	37.5	37.5
t (mm)	0.375	0.750	1.500	0.375	0.750	1.500	0.375	0.750	1.500

Table 3
Mesh parameters of numerical models.

Type of elements	C3D15/C3D20R
Number of elements	54,724–61,398
Hexahedral	35,532–40,532
Wedge	18,168–21,458
Number of nodes	998,520–1,084,720
Hexahedral	710,640–810,640
Wedge	272,520–321,870
Degrees of freedom	2,995,560–3,254,160
Hexahedral	2,131,920–2,431,920
Wedge	817,560–965,610
Max. element edge length	0.862 mm

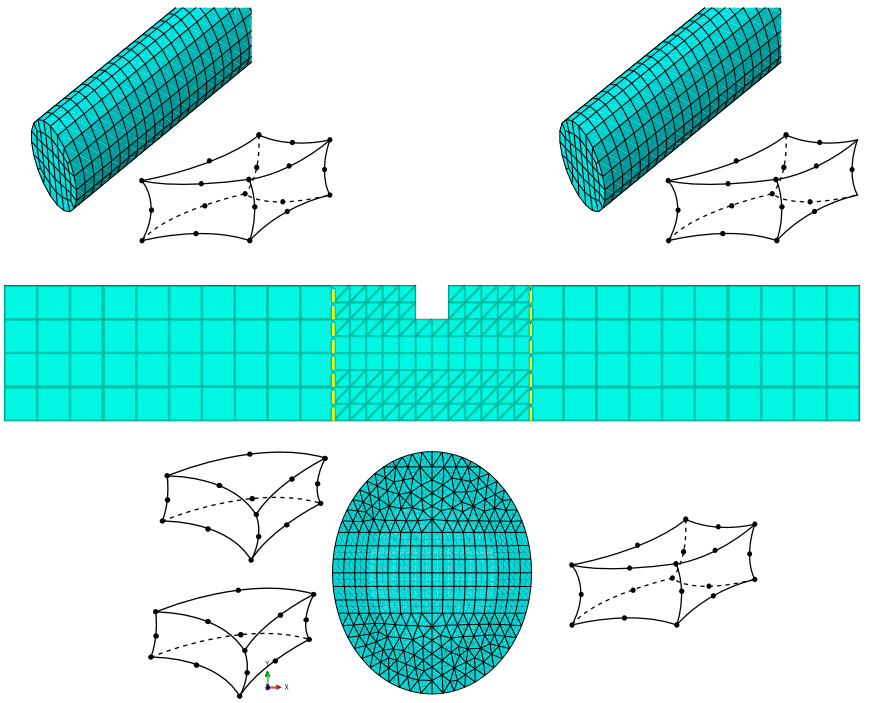

Fig. 2. Mesh description.

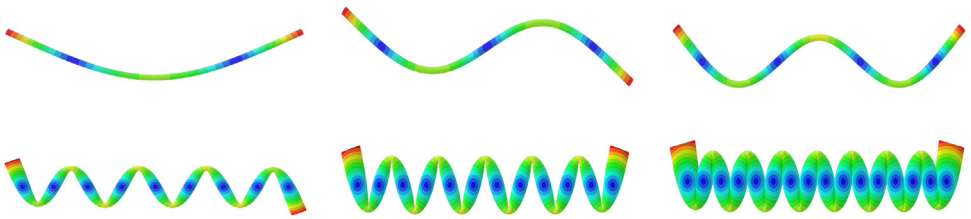

Fig. 3. Selected bending mode shapes (modes 1, 3, 5, 15, 21 and 29) of the numerical modal analysis; in the undamaged case the modes appear in pairs, with the same eigenfrequency applying to two modes with identical shape except one is rotated 90° around the axis of the cylinder relative to the other.

Table 4
Numerically calculated eigenfrequency of all 30 identified bending mode shapes for the undamaged model.

Mode number	1/2	3/4	5/6	7/8	9/10
Frequency (Hz)	371.21	1021.37	1996.92	3289.32	4892.20
Mode number	11/12	13/14	15/16	17/18	19/20
Frequency (Hz)	6797.6	8996.43	11,478.54	14,233.08	17,248.57
Mode number	21/22	23/24	25/26	27/28	29/30
Frequency (Hz)	20,513.13	24,014.64	27,740.91	31,679.78	35,819.28

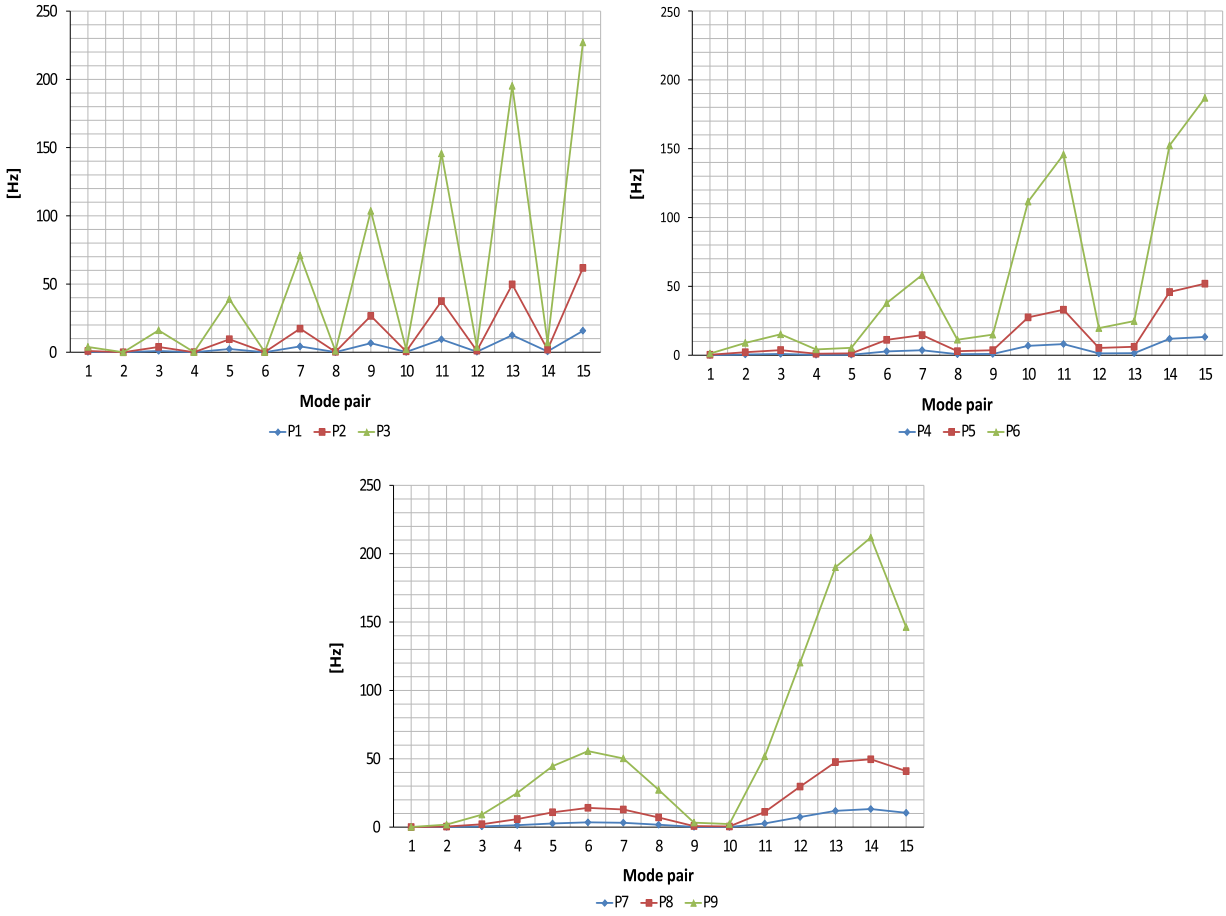

Fig. 4. Magnitude of the shift in the numerically determined eigenfrequencies for the first 15 bending mode shape pairs (models 1–3, 4–6 and 7–9).

Table 3 presents the mesh specifications of the numerical models including type of elements, number of elements and nodes, degrees of freedom and maximum element edge length. The range of values presented account for slight variations in the final mesh of the nine finite element models. The variation is less than 10 percent across all models.

Fig. 3 shows the mode shapes 1, 3, 5, 15, 21 and 29. The corresponding eigenfrequencies of all modes for the undamaged model are presented in Table 4.

Fig. 4 displays the magnitude of the shift in eigenfrequencies over the 15 mode shape pairs found in the FEM for the nine damaged models compared to the undamaged model in Table 4.

When comparing damage-induced eigenfrequency changes with tolerance-induced eigenfrequency changes, it can be noticed that possible deviations in form, material or geometry influence all eigenfrequencies equally. Whereas cracks change, depending on size and position, the eigenfrequencies of the observed modes differently.

5. Experiments

The main challenges of the experiments were to create a short intense impulse to excite the specimen in the intended bandwidth and the preparation of supporting conditions for repeatable measurements. Fig. 5 presents the experimental setup. The sample holder is placed on a vibration isolated table in order to exclude structural vibration induced by the foundation. The three main components of the setup are:

- the excitation unit that contains an electrodynamical shaker. After a transient signal the vibration of the test specimens decays freely,
- a signal transfer system that captures excitation force and duration. At the output side a Laser-Scanning-Vibrometer measures normal surface velocities on the test specimens and
- an analyzer unit digitizes the time signal, processes and visualizes the captured data.

As shown in Fig. 5(b) the ends of the test specimens are placed on a foam padding to approximate free–free boundary conditions.

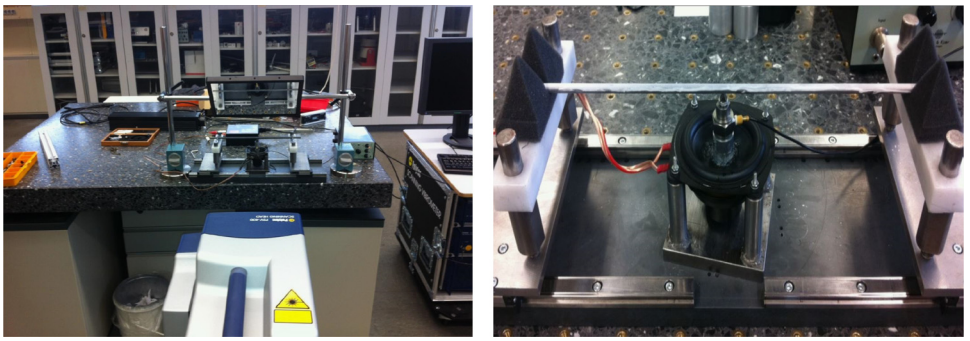

Fig. 5. Left: general measurement setup and right: support conditions and excitation unit.

The Laser-Scanning-Vibrometer PSV400 is employed to measure surface velocities at 39 points of each mass centroid axes and a shaker with a high dynamic range is used for a broadband excitation. ME'Scope V5 is used as a post-processing software to extract the eigenvectors and eigenfrequencies from the measured data.

Table 5 illustrates the parameters for the experiments.

Table 5
Experiment parameters.

Parameter Quantity	Bandwidth $f_{max} = 40$ kHz	Sampling rate $f_s = 102.4$ kHz	FFT-lines $n_{FFT} = 819,200$
Parameter Quantity	Resolution $\Delta f = 0.125$ Hz	Block size $T_s = 8$ s	Averaging $n_A = 3$
Parameter Quantity	Pretrigger $10\% \cdot T_s$	Window source Force [33]	Window LDV Exponential [33]

6. Model validation

From a mechanical point of view, real structures possess an infinite number of degrees of freedom (DOF). Due to practical reasons the response to an excitation is only measurable at a finite number of locations. Usually, the number of

measurement points, m, is much smaller than the number of numerically modeled DOFs, n. Advances in computational power allow numerical models with millions of DOFs to be solved within an acceptable time frame. However, engineers are faced with the choice of adjusting the numerical model to the experiment (modal reduction) or vice versa (modal expansion) [10]. In this study, a modal reduction strategy is utilized, in which the numerical model is adapted to the experiment where 39 measurement points are used. The calculated results of the numerical model are transferred to master-nodes with the same geometric position and DOFs as measured in the experiment. Furthermore, a mode-tracking procedure [11] is implemented to consider possible mode shifts due to the varying crack parameters.

After ensuring the availability of numerically calculated and experimentally determined eigenvectors of coincident position, modal validation is performed. In this work, the Modal Assurance Criterion (MAC) [12,13] is used to verify correlation between numerically calculated and experimentally determined eigenvectors. The MAC is given by

$$\mathrm{MAC} = \frac{(\phi_m^T \phi_n)^2}{(\phi_m^T \phi_m)(\phi_n^T \phi_n)}, \tag{4}$$

where ϕ_m and ϕ_n are two vectors to compare. The MAC can attain values between 0 (the two vectors are uncorrelated) and 1 (the two vectors are linear dependent). In this study, the MAC-values of the main diagonal in the MAC-matrix are between 0.78 and 0.98. Side entries account for values between 0.01 and 0.08, when comparing experimental and numerical results.

If the experimental data serve as reference, one strives for the validation of modal assumptions and boundary conditions. Possible deviations between numerical and experimental results can be explained due to the uncertainties of elastic material parameters or the elastic support. To reduce these deviations, an elastic support is included in the numerical model and Young's modulus of the simulated material is updated manually. These steps consequently increase the predictive precision in the process of damage identification. Fig. 6 shows the boundary conditions in the simulation and the experiment.

Fig. 7 depicts the maximum and mean deviation between experimentally determined and numerically calculated eigenfrequencies for all nine test objects over the mode number including an elastic support and updating Young's modulus. The lower eigenfrequencies are more affected by the support conditions than the higher eigenfrequencies. Therefore, the maximum and mean deviation decreases with increasing mode rank.

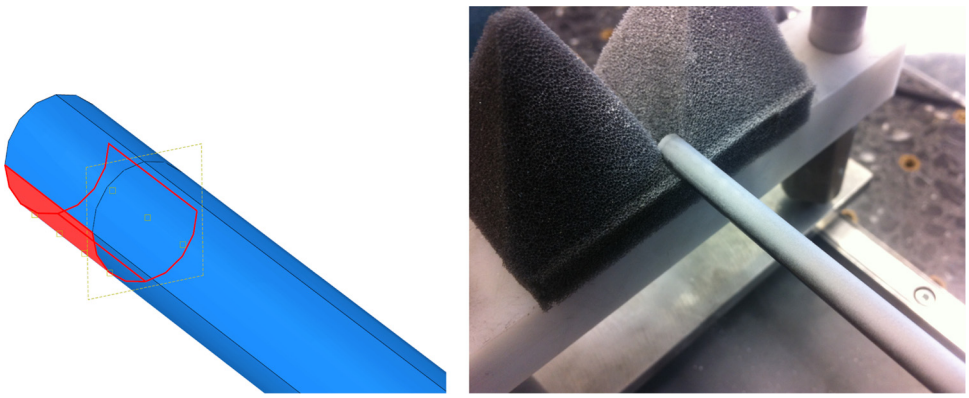

Fig. 6. Left: section of modeled elastic foundation and right: foam padding as flexible support.

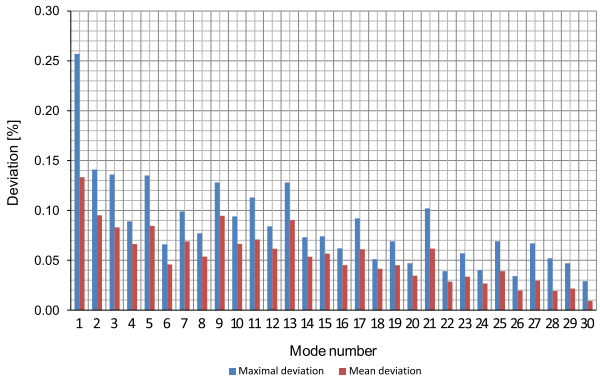

Fig. 7. Maximum and mean deviation between numerically calculated and experimentally determined eigenfrequencies for the nine test objects over the mode number.

7. Results of damage identification

In Figs. 8–11 the objective function values are plotted. The visualization helps us to understand the shape of search space in which appropriate initial vectors for the identification routine can be found quickly.

The compiled objective function plots visualize the complete search space for crack position y_0 and crack depth t. The graph depicts the values of objective function cf. Eq. (3) for the specific eigenfrequency combination which is chosen. Green denotes a small, yellow a mid-level and red a high objective function value on a normalized scale. To connect the results of damage identification with the objective function plots, the outcome of the particular damage identification and the real crack position and depth are shown. Therein crosses denote the position of the real crack parameters and circles the results of damage identification.

The objective function involving the first four eigenfrequencies takes the form

$$f(\vartheta) = \sum_{i=1}^{4} \frac{(f_{\exp_i} - f_{\mathrm{num}_i})^2}{f_{\exp_i}^{\,2}}. \tag{5}$$

Table 6 contains the damage identification results for the first three test objects with eigenfrequencies 1–4 used to define the objective function. The numerically predicted crack depth t was between 10.08 and 13.43 percent of the actual crack depth of the test specimens. The predicted crack position y_0 was between 0.58 and1.90 percent of the actual crack position. The crack of test object 1 is not identified. Convergence is achieved after 9–12 iterations.

An objective function that involves global modal data, i.e. eigenfrequencies of lower modes yields results of damage identification which are not very precise. It is assumed that this is related to the higher deviations of eigenfrequencies, cf. Fig. 7, compared to the eigenfrequencies of higher mode rank which contain more local information. Additionally if utilizing eigenfrequencies of lower rank, one fails to identify small damage levels cf. test object 1. Whereas by involving global modal data the computational time decreases due to the more homogeneous search space in comparison to eigenfrequencies of local modes.

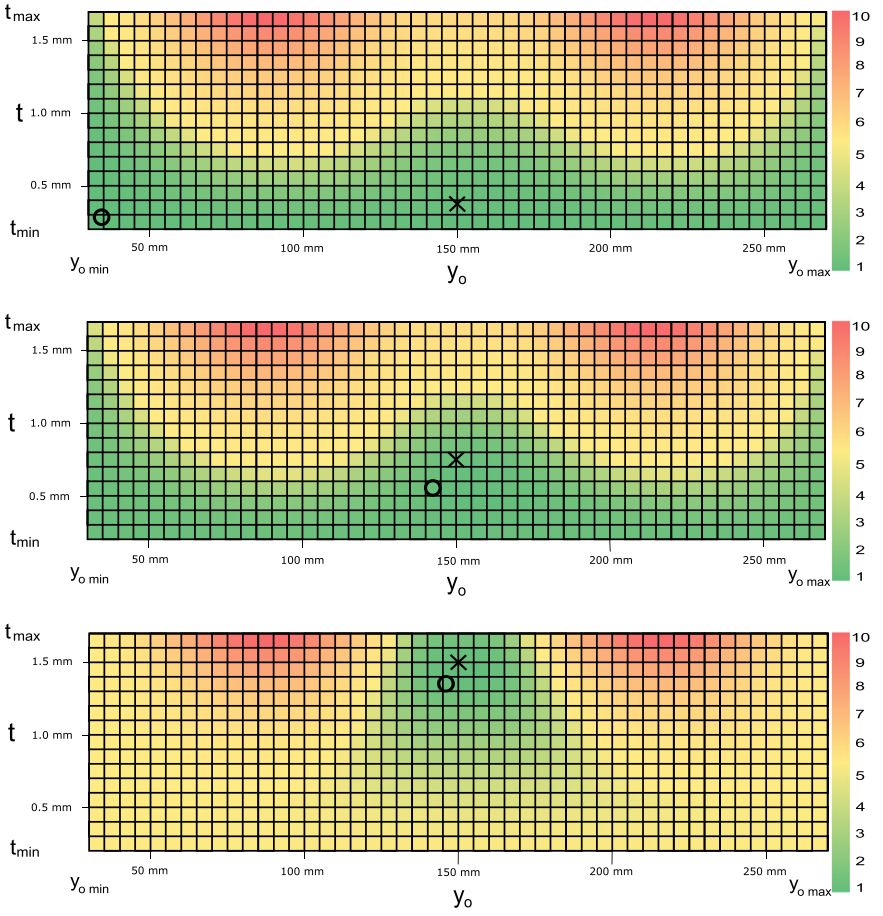

Fig. 8. Objective function plots for test objects 1–3 involving the eigenfrequencies 1–4 (crosses denote the real parameter vectors and circles computed parameter vectors). (For interpretation of the references to color in this figure caption, the reader is referred to the web version of this paper.)

Table 6
Results of damage identification (test objects 1–3 involving eigenfrequencies 1–4).

Test object	1	2	3
t_{real} (mm)	0.38	0.75	1.50
t_{opt} (mm)	–	0.54	1.34
%-dev.	–	13.43	10.08
y_{0real} (mm)	150.00	150.00	150.00
y_{0opt} (mm)	–	144.88	148.44
%-dev.	–	1.90	0.58

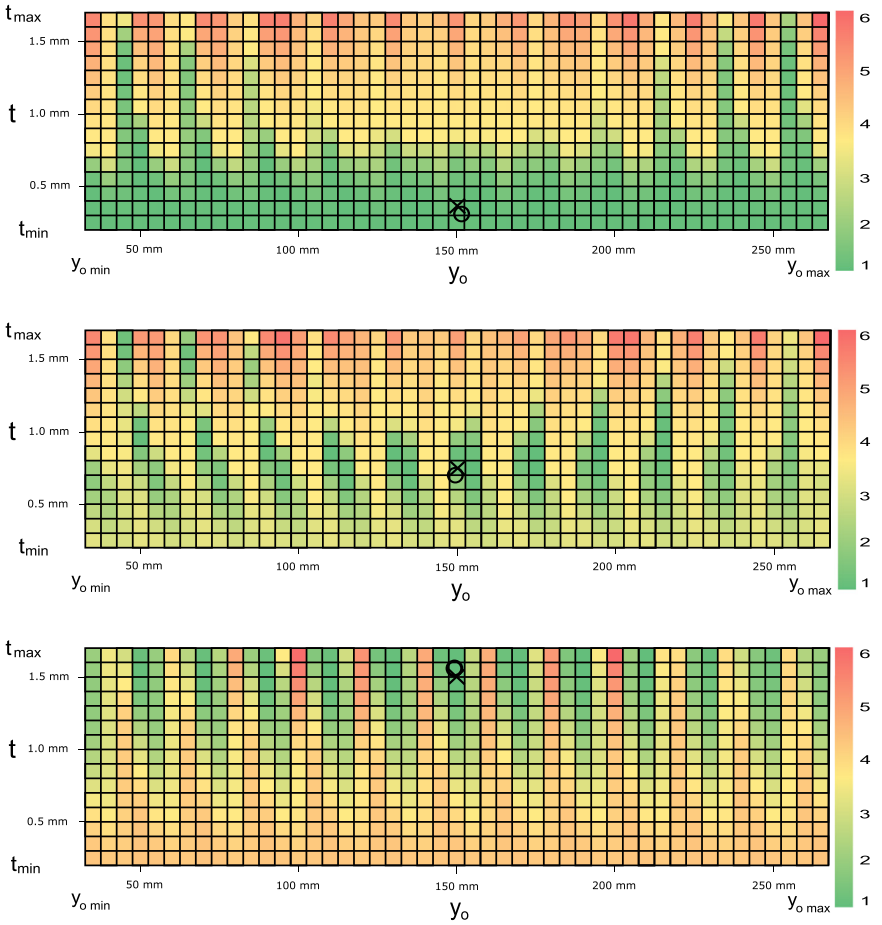

Fig. 9. Objective function plots for test objects 1–3 involving the eigenfrequencies 27–30 (crosses denote the real parameter vectors and circles computed parameter vectors). (For interpretation of the references to color in this figure caption, the reader is referred to the web version of this paper.)

Table 7
Results of damage identification (test objects 1–9 involving eigenfrequencies 27–30).

Test object	1	2	3	4	5	6	7	8	9
t_{real} (mm)	0.38	0.75	1.50	0.38	0.75	1.50	0.38	0.75	1.50
t_{opt} (mm)	0.31	0.70	1.55	0.43	0.73	1.49	0.32	0.63	1.61
%-dev.	4.26	3.29	3.29	3.48	1.23	0.97	3.81	7.61	7.10
y_{0real} (mm)	150.00	150.00	150.00	75.00	75.00	75.00	37.50	37.50	37.50
y_{0opt} (mm)	150.76	149.42	149.46	75.45	74.88	75.29	37.96	38.23	37.86
%-dev.	0.28	0.22	0.20	0.17	0.05	0.11	0.17	0.27	0.13

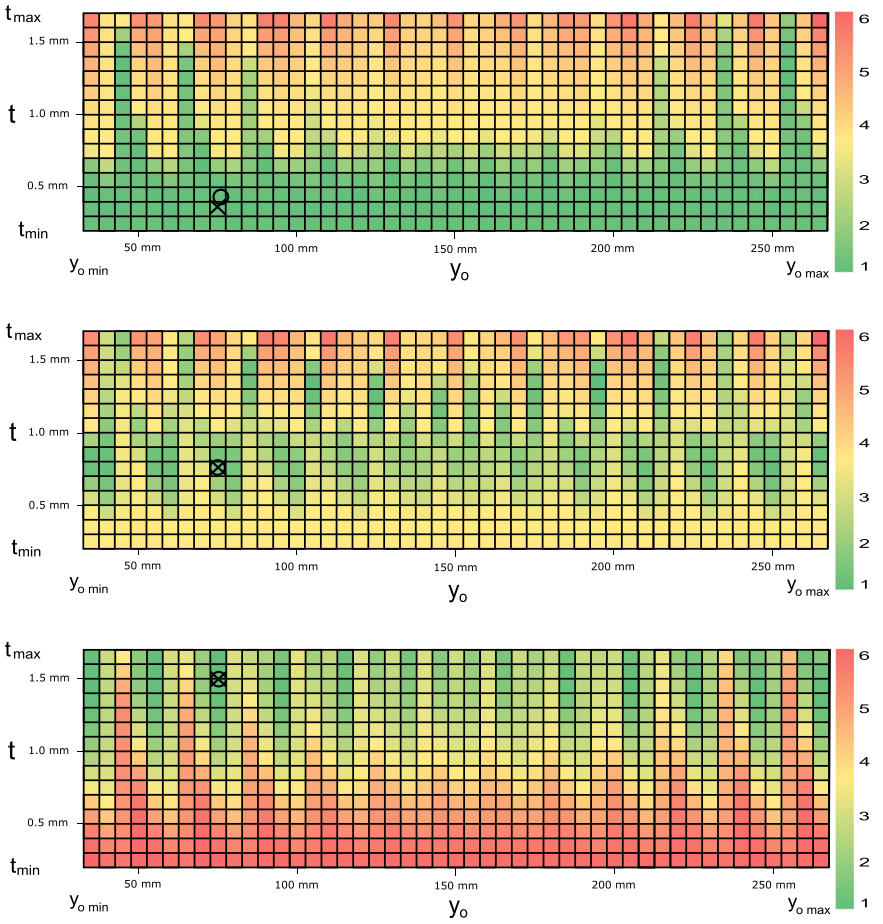

Fig. 10. Objective function plots for test objects 4–6 involving the eigenfrequencies 27–30 (crosses denote the real parameter vectors and circles computed parameter vectors). (For interpretation of the references to color in this figure caption, the reader is referred to the web version of this paper.)

Due to the larger characteristic mode shape length, global modes are less sensitive to small defects compared to local modes. Hence, the eigenfrequencies of local modes are used in the optimization procedure. The four highest eigenfrequencies are chosen in the objective function to detect the smallest damage levels ($t = 0.375$ mm):

$$f(\vartheta) = \sum_{i=27}^{30} \frac{(f_{\exp_i} - f_{\mathrm{num}_i})^2}{f_{\exp_i}^{\,2}} \tag{6}$$

follows from Eq. (3). Table 7 contains the damage identification results for the nine test objects with eigenfrequencies 27–30 used to define the objective function.

The numerically predicted crack depth t was between 0.97 and 7.61 percent of the actual crack depth of the test specimens. The predicted crack position y_0 was between 0.05 and 0.28 percent of the actual crack position. The test objects five and six show the most precise results in damage identification due to the smallest deviations of eigenfrequencies. Convergence is achieved after 12–20 iterations.

Utilizing eigenfrequencies of higher mode rank has the advantage of more precise results in damage identification due to the lower deviations of eigenfrequencies, cf. Fig. 7 compared to the eigenfrequencies of global modes. Additionally if involving eigenfrequencies of higher mode rank, one is able to identify small damage levels. Whereas by involving local modal data the computational time increases due to the less homogeneous search space in comparison to global modes.

Without the exhaustive search on the course gridded plots, the optimization fails or requires a higher number of iterations (20–30) compared to the suggested procedure (9–20). This fact has to be taken into account, if one considers that an iteration takes 40 min on a PC with the specifications of a 64-bit Windows machine with 16 cores at 2.53 GHz and 24 GByte RAM.

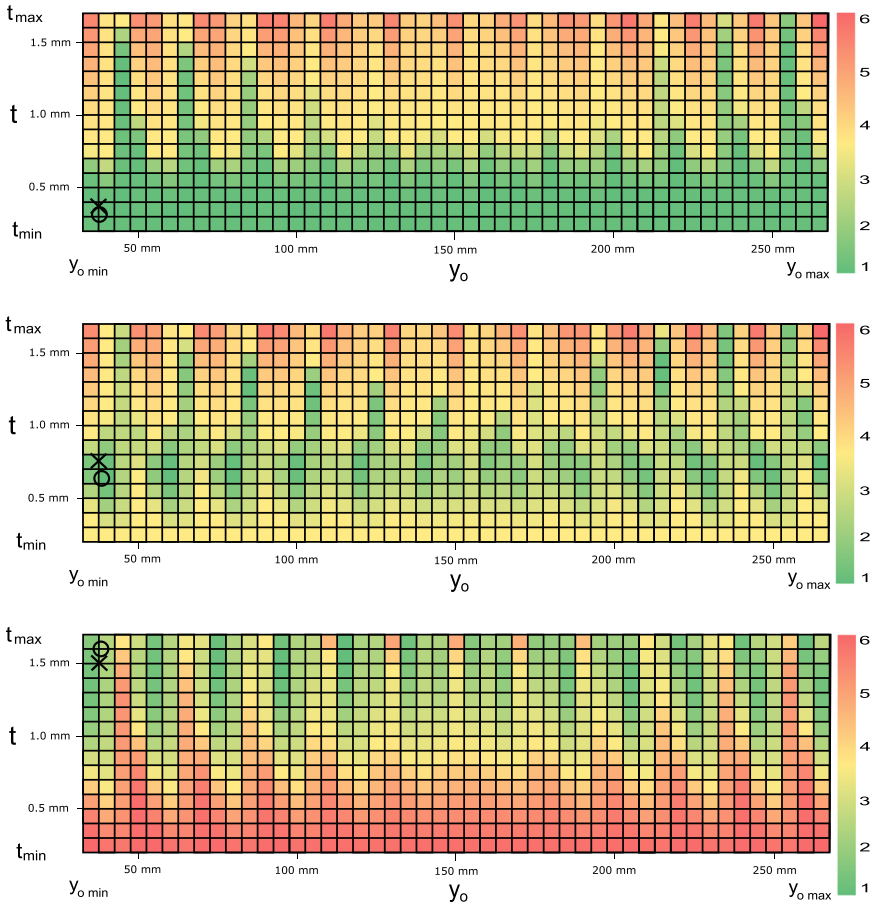

Fig. 11. Objective function plots for test objects 7–9 involving the eigenfrequencies 27–30 (crosses denote the real parameter vectors and circles computed parameter vectors). (For interpretation of the references to color in this figure caption, the reader is referred to the web version of this paper.)

8. Final remarks

In the presented study a damage identification technique based on modal data of long and slender structures is presented. Numerically calculated and experimentally determined eigenvectors and eigenfrequencies are used to compute geometrical crack parameters.

It is demonstrated that for detecting small damage levels, such as crack depth/diameter ratios less than 10 percent, it is essential to involve modal data of local modes with adequate measurement precision. As expected, the precision of the damage identification procedure increases when the deviation between numerically computed and experimentally determined eigenfrequencies are small.

The lowering of computational time, but maintaining the attained precision, presents the main goal of future work. This can be achieved by using fewer elements, substituting the utilized meshes with elements of lower node quantity or increasing the computational power.

Suitable initial values for the crack parameters are important for the success of the presented method. As there is no a priori knowledge of crack position in real testing scenarios, further investigation is required to determine a generally valid approach for initial parameter selection.

One drawback related to damage identification based on eigenfrequencies is when symmetrical structures are investigated. The crack has two potential positions with the same distance to the central axis. Therefore it is suggested to connect global methods with high resolution local methods such as ultrasonic testing or eigenvector extraction with a sufficient spatial resolution. Considering ultrasonic techniques, difficulties can arise from small object diameters and the consequent short sound paths, which makes reliable assessment of structural integrity difficult. High resolution measurements of eigenvector data represents an alternate approach to overcome the non-uniqueness. The main disadvantages of this approach are the slower data extraction compared to global methods and the insensitivity to small damage levels [31].

In light of the increasing usage of composites in all technical sectors, engineers are faced with the challenge to apply vibration based damage identification methods to parts with high structural damping. This is accompanied by difficulties in the modal analysis of highly damped materials, which in turn prevents the identification of small damage levels.

References

[1] G.M.L. Gladwell, The inverse problem for the vibrating beam, *Proceedings of the Royal Society of London* 393 (1984) 277–295.
[2] A. Morassi, A uniqueness result on crack location in vibrating rods, *Inverse Problems in Engineering* 4 (1997) 231–254.
[3] F. Vestroni, D. Capecchi, Damage evaluation in cracked vibrating beams using experimental frequencies and finite element models, *Journal of Vibration and Control* 2 (1996) 69–86.
[4] F. Vestroni, D. Capecchi, Damage detection in beam structures based on frequency measurements, *Journal of Engineering Mechanics* 126 (2000) 761–768.
[5] G.M.L. Gladwell, *Inverse Problems in Vibration*, Kluwer Academic Publisher, Dordrecht, The Netherlands, 2004.
[6] M.I. Friswell, Damage identification using inverse methods, *Proceedings of the Royal Society of London* 365 (2007) 393–410.
[7] M.I. Friswell, J.E. Mottershead, Inverse methods in structural health monitoring, *Key Engineering Materials* 204–205 (2001) 201–210.
[8] C.R. Farrar, S.W. Doebling, D.A. Nix, Vibration-based structural damage identification, *Philosophical Transactions of the Royal Society of London* 359 (2001) 131–149.
[9] ABAQUS 6.13, *Abaqus/CAE User Guide*, 2013.
[10] M.I. Friswell, J.E. Mottershead, *Finite Element Model Updating in Structural Dynamics*, Kluwer Academic Publishers, Dordrecht, The Netherlands, 1995.
[11] T.S. Kim, Y.Y. Kim, Mac-based mode-tracking in structural topology optimization, *Computers and Structures* 74 (2000) 375–383.
[12] R. J. Allemang, The modal Assurance Critrion—Twenty Years of use and Abuse, *The 20th International Modal Analysis Conference*, 2002.
[13] M. Pastor, M. Binda, T. Harcarik, Modal assurance criterion, *Procedia Engineering* 48 (2012) 543–548.
[14] ABAQUS 6.13, *Analysis User Guide Volume V: Prescribed Conditions, Constraints and Interactions*, 2013.
[15] L. Harzheim, *Strukturoptimierung Grundlagen und Anwendungen*, Harri Deutsch, Frankfurt am Main, Germany, 2008.
[16] K. Svanberg, The method of moving asymptotes—a new method for structural optimization, *International Journal for Numerical Methods in Engineering* 24 (1987) 359–373.
[17] S. Marburg, Developments in structural-acoustic optimization for passive noise control, *Archives of Computational Methods in Engineering* 9 (4) (2002) 291–370.
[18] M.H. Houten, *Function Approximation Concepts for Multidisciplinary Design Optimization*, 1998.
[19] M.I. Friswell, J.E.T. Penny, Is damage location using vibration measurements practical?, *Proceedings of Euromech 365 International Workshop*, 1997.
[20] A. Alvandi, C. Cremona, Assessment of vibration-based damage identification techniques, *Journal of Sound and Vibration* 292 (2006) 179–202.
[21] F.S. Buezas, M.B. Rosales, C.P. Filipich, Damage detection with genetic algorithms taking into account a crack contact model, *Enginieering Fracture Mechanics* 78 (2011) 695–712.
[22] K.J. Aström, P. Eykhoff, System identification—a survey, *Automatica* 7 (1971) 123–162.
[23] R. Serban, J.S. Freeman, Identification and identifiability of unknown parameters in multibody dynamic systems, *Multibody System Dynamics* 5 (2001) 335–350.
[24] L. Ljung, G. Jordan, *System Identification: Theory for the User*, Prentice-Hall, Englewood Cliffs, USA, 1987.
[25] J.A. Jacquez, P. Greif, Numerical paramter identifiability, estimability and optimal sampling design, *Mathematical Bioscience* 77 (1985) 201–227.
[26] B.C. Moore, Principal component analysis in linear systems: *controllability, observability and model reduction*, *IEEE Transactions on Automatic Control* 26 (1981) 17–32.
[27] A. Raue, C. Kreutz, T. Maiwald, U. Klingmueller, J. Timmer, Addressing parameter identifiability by model-based experimentation, *IET Systems Biology* 5 (2) (2011) 120–130.
[28] R. Bellmann, K.J. Astroem, On structural identifiability, *Mathematical Bioscience* 7 (3–4) (1970) 329–339.
[29] C.C. Travis, G. Haddock, On structural Identification, *Mathematical Bioscience* 56 (3–4) (1981) 157–173.
[30] M. Ranjbar, H.-J. Hardtke, D. Fritze, S. Marburg, Finding the best design within limited time: *a comparative case study on methods for optimization in structural acoustics*, *Journal of Computational Acoustics* 18 (2) (2010) 149–164.
[31] W. Fan, P. Qiao, Vibration-based damage identification methods: *a review and comparative study*, *Structural Health Monitoring* 10 (1) (2010) 83–111.
[32] S. Marburg, H-J. Hardtke, Shape optimization of a vehicle hat-shelf improving acoustic properties for different load cases by maximizing first eigenfrequency, *Computers and Structures* 79 (2001) 1943–1957.
[33] Polytec, *User Guide*, 2010.